Calculation of the electronic properties of Ni-P amorphous alloys

Hyungjin Yang
Department of Physics, Indiana University, Bloomington, Indiana 47405

James C. Swihart
Department of Physics, Indiana University, Bloomington, Indiana 47405

Donald M. Nicholson
Oak Ridge National Laboratory, Oak Ridge, Tennessee 37831

Randall H. Brown
Department of Physics, Luther College, Decorah, Iowa 52101
(Received 13 April 1992; revised manuscript received 6 August 1992)

We have simulated the atomic structure of Ni-P amorphous alloys for several concentrations ($Ni_{75}P_{25}$, $Ni_{80}P_{20}$, and $Ni_{85}P_{15}$), and have calculated their electronic properties. The atoms are spread randomly in a periodically repeated cell and then relaxed using Weber-Stillinger pair potentials to a local minimum potential energy. We have constructed eight such cells for each concentration. Because the unit cell (80 or 160 atoms) is larger than the electronic mean free path, we can assume the electronic properties are independent of boundary conditions. We impose periodic boundary conditions, which is equivalent to calculating the band structure at $\mathbf{k}=0$ of the periodically extended unit cell. Using linearized Korringa-Kohn-Rostoker (KKR) band theory, we have calculated the total density of states, component- and angular-momentum-decomposed densities of states, degree of localization, and current matrix elements for the electrons. We find very little localization of the electrons near the Fermi energy. We also have calculated the electrical resistivity and reflectivity as a function of frequency and concentration using the Kubo formula. Finally we have compared our calculated results with experiment and with results obtained from the effective-medium approximation and from the KKR coherent-potential approximation.

I. INTRODUCTION

Ni-P amorphous alloys are readily formed by rapid cooling of the liquid. In this state, long-range order is absent; i.e., the system does not have a lattice structure, and the quenched state is a local minimum in energy. The only structural information available from experiment is the pair correlation (distribution) functions. This lack of information about the structure and the absence of a standard band theory requires the construction of approximate models that represent the amorphous structure. We model the system by a supercell, which allows us to apply band theory. If the supercell is large enough (for example, much larger than a mean free path), it seems reasonable to expect that our model will have the same electronic properties as the amorphous metal independent of the boundary conditions we impose on the supercell. Thus, we apply periodic boundary conditions, which for the electronic properties is equivalent to carrying out a band-structure calculation confined to the one k point at $\mathbf{k}=\mathbf{0}$.

It is known that the mean free path for the Ni-P amorphous alloys is of the order of the interparticle separation. For 160 atoms in a cubic unit cell, the mean free path is a little less than $\frac{1}{5}$ the length of a cell edge. Therefore, periodic boundary conditions should not seriously affect the calculated electronic properties of the Ni-P amorphous alloy system when the supercell is this large.

We have simulated eight Ni-P amorphous alloy samples at each concentration: $Ni_{75}P_{25}$, $Ni_{80}P_{20}$, and $Ni_{85}P_{15}$. We picked these concentrations, since amorphous Ni-P alloys can be formed in the range of 15–26 at. % phosphorus.[1] The atomic concentration of phosphorus at the eutectic point is 19%.[2]

The general goal of this work is to calculate electronic properties of the Ni-P amorphous alloy system, which is representative of transition metal-metalloid glasses. Structural,[3] electronic,[4] magnetic,[5] optical,[6] and transport properties[7] of the Ni-P system have been measured. Various theoretical models[8] have been proposed and several theoretical calculations[9–11] have been done. However, to our knowledge there are no calculations of the electrical resistivity as a function of concentration for the Ni-P met glasses. Experiments show a rather large change in resistivity with concentration. One of the goals of the present work is to study this resistivity change theoretically.

In Sec. II, we describe the construction of the supercell model of the amorphous alloy. In Sec. III, we discuss the band-structure calculations for the electronic structure. In Sec. IV, we present results for the electronic structure as well as the electrical resistivity and reflectivity at zero temperature as a function of concentration. In addition to comparing our results with experiment, we compare also with the results for $Ni_{80}P_{20}$ obtained from the effective-medium approximation (EMA) and from the Korringa-Kohn-Rostoker coherent-potential approxima-

tion (KKR-CPA) using the same potentials as those used in our simulated supercell calculations. In the KKR-CPA calculations, one assumes the material is a random substitutional alloy with the atoms on a lattice rather than an amorphous alloy.

II. COMPUTER SIMULATION OF AMORPHOUS Ni-P ALLOYS

We construct our computer-simulated unit cell with periodic boundary conditions for 80 or 160 atoms. We have constructed four such samples at each of the three concentrations and at each of the total numbers of 80 and 160.

In the first stage of our simulation, we use a random number generator to distribute the atoms randomly in the periodically repeated supercell. We use a hard-sphere interatomic potential, so that the atoms do not overlap.

In the second stage, we use effective pair potentials (Ni-Ni, Ni-P, and P-P) (Ref. 12) in place of the hard-sphere potential used in the first stage. At the beginning of this stage, we determine randomly which atoms are Ni and which atoms are P. But in Ni-P amorphous alloys, experiment shows that metalloid atoms do not contact each other.[13] In our simulation, close contact between metalloid atoms is avoided by interchanging a Ni and a P when two P atoms are too close. We now rearrange the positions of the atoms and adjust the density to obtain a local minimum in the total potential energy.[14]

The partial pair distribution functions averaged over the four 160 atom samples of $Ni_{80}P_{20}$ are compared with experiment[13] in Fig. 1. The unphysical oscillations in the experimental data at small r have been suppressed. There is excellent agreement between the calculated and experimental results for the Ni-Ni pair distribution. For the Ni-P, there are fewer pairs than for Ni-Ni. Hence, although there is good agreement between our calculation and experiment for this case, as would be expected, the agreement is not quite as good as with the Ni-Ni distribution function. Because of the small number of P-P pairs in our model samples, the calculated P-P distribution function is noisy. However it agrees with experiment in that the P-P pairs are farther apart than the Ni-P and Ni-Ni pairs. This is seen by the fact that the first peak in the P-P distribution occurs at larger r than does the first peak for the other two distributions.

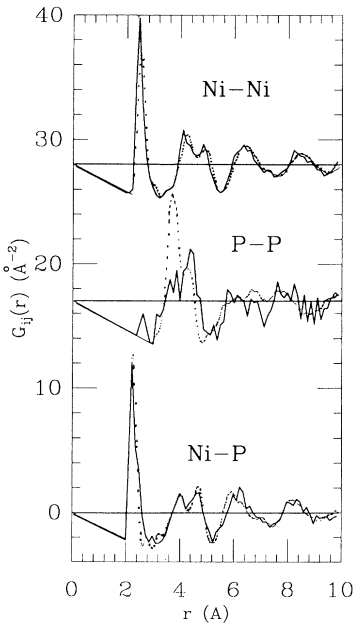

FIG. 1. Comparison of the experimentally measured partial pair distribution functions for $Ni_{80}P_{20}$ (Ref. 13) (dotted line) with the calculated results (solid line), which are the average of four computer generated samples with 160 atoms each, as a function of radial separation. Note that although the calculated P-P curve is noisy, it does show, in agreement with experiment, that for our model the phosphorus atoms are not close to each other.

III. BAND THEORY FOR THE SUPERCELL

In calculating the electronic properties, we use the one-electron model with spherical muffin-tin potentials in which exchange and correlation are treated in the local-density approximation (LDA). We scale the dimensions of the supercell so that we have an atomic volume of 75.87 a.u.^{3} in each case. This corresponds to densities of 8.06, 7.85, and 7.65gm/cm^3 for $Ni_{85}P_{15}$, $Ni_{80}P_{20}$, and $Ni_{75}P_{25}$, respectively. These values are close to the experimental densities. In constructing our supercell and setting its density equal to experimental values, we are proceeding in the same way as for doing a band-structure calculation on a perfect crystal in which the crystal structure and lattice constants are set to agree with experiment.

With 160 atoms in a unit cell, the band-structure calculation is a large numerical calculation even when restricted to $\mathbf{k}=0$. We use linearized Korringa-Kohn-Rostoker (LKKR) band theory,[15] with the angular-momentum decomposition of the spherical muffin-tin potentials cut off at $l_{\max}=2$. The potentials are ones that were determined self-consistently at each concentration in a KKR-CPA calculation. In the KKR-CPA calculation, the atoms were assumed to be distributed at random on an fcc lattice with the experimental density of the amorphous alloy. Thus the potentials are not determined self-consistently for the amorphous-alloy calculation. However, we expect these potentials to be reasonable approximations to the self-consistent potentials of the amorphous system.

A major advantage of the LKKR approach is that all the eigenvalues and eigenvectors (for a range of energies) for a given k vector are obtained from one matrix diagonalization. Using LKKR code reduces the computer time by the order of 100 compared to full KKR calculations.

Further simplification is possible for the supercell calculation because, with periodic boundary conditions, the band structure needs only be calculated at $\mathbf{k}=\mathbf{0}$. The one k point calculation reduces again the computation time by the order of 100. Our one k point LKKR band calculation is, therefore, of the order of 10 000 times faster than calculating the full KKR band structure. In spite of

its rapid convergence, the CPU time to complete the LKKR calculation for one sample at $\mathbf{k}=0$ is about 3600 CPU seconds using the CRAY-2 when we have 160 atoms in the unit cell and include angular-momentum-decomposed eigenfunctions up to $l=2$.

IV. RESULTS OF ELECTRONIC PROPERTY CALCULATIONS

We have calculated a number of the electronic properties including the total density of states, constituent and angular-momentum-decomposed density of states, degree of localization of eigenstates, and average number of electrons at the Ni and P sites. We have also calculated the electrical resistivity and reflectivity as a function of frequency for each of the three concentrations. We find that we obtain nearly the same results for the electronic densities of states (DOS) and for the location of the Fermi energy E_f for the 80 atom samples and for the 160 atom samples. The value of E_f differs by only a few tenths of a percent between the two sizes of cell, while the DOS at E_f differs by about 10%. The shape of the DOS with energy is almost identical for the 80 and 160 atom cases.[16]

Our calculated (DOS) (averaged over four configurations of 160 atoms each for each concentration) for $Ni_{80}P_{20}$ and for $Ni_{75}P_{25}$ are compared with experimentally measured photoemission spectra[17,18] in Figs. 2(a) and 2(b). In Fig. 2(a), the experimental data[17] are for amorphous $Ni_{79}P_{21}$ taken at 300 K. In Fig. 2(b), the experiment[18] is for *crystalline* Ni_3P. The photoemission spectral data are in arbitrary units. Therefore, in Figs. 2 we have adjusted the height of the peaks in the experimental data to coincide approximately with the peaks in our DOS calculations. In these figures, we have set our calculated Fermi energy equal to the experimental Fermi energy as given in the experimental papers.[17,18] The energy scale is then fixed for both the experimental and calculated curves. One may question whether comparing with data on a crystalline sample in Fig. 2(b) is reasonable. However in Ref. 18, data is also given for an amorphous sample of $Ni_{78}P_{14}B_8$, and the curve is nearly identical to the Ni_3P data, at least in the neighborhood of the large peak from the Ni d band. Thus one sees that the spectrum is dominated by the Ni d electrons, and the shape near the peak is nearly independent of whether the sample is in the amorphous or crystalline state. The spectrum near the peak also seems to be relatively insensitive to the substitution of a small amount of boron for some of the phosphorus.

The location of the Fermi energy for Ni_3P in Ref. 18 at about the midpoint of the steeply falling spectrum just above the major peak seems reasonable. However, the location of E_F in $Ni_{79}P_{21}$ as indicated by Thube *et al.*[17] [and as shown in Fig. 2(a)] seems to us to be too near the peak. In fact, in their Fig. 2, they show E_F for $Ni_{89}P_{11}$ as being below the photoemission peak. This does not make any sense to us for x-ray photoemission spectroscopy data at 300 K.

We see that the location and shape of the peak is nearly the same for experiment and calculation at both concentrations. If we would shift the Fermi energy 0.08 Ry higher for the $Ni_{79}P_{21}$ experimental data [i.e., shift the experimental curve to the left 0.08 Ry in Fig. 2(a)], then E_F would be at the midpoint of the rapidly falling part of the DOS, and there would be better agreement between our calculated curve and the experimental curve. There is some deviation between the two curves at lower energies, which remains even with a shift in E_F, but such a deviation is not unexpected, since the photoemission data depend on matrix elements as well as on the DOS.

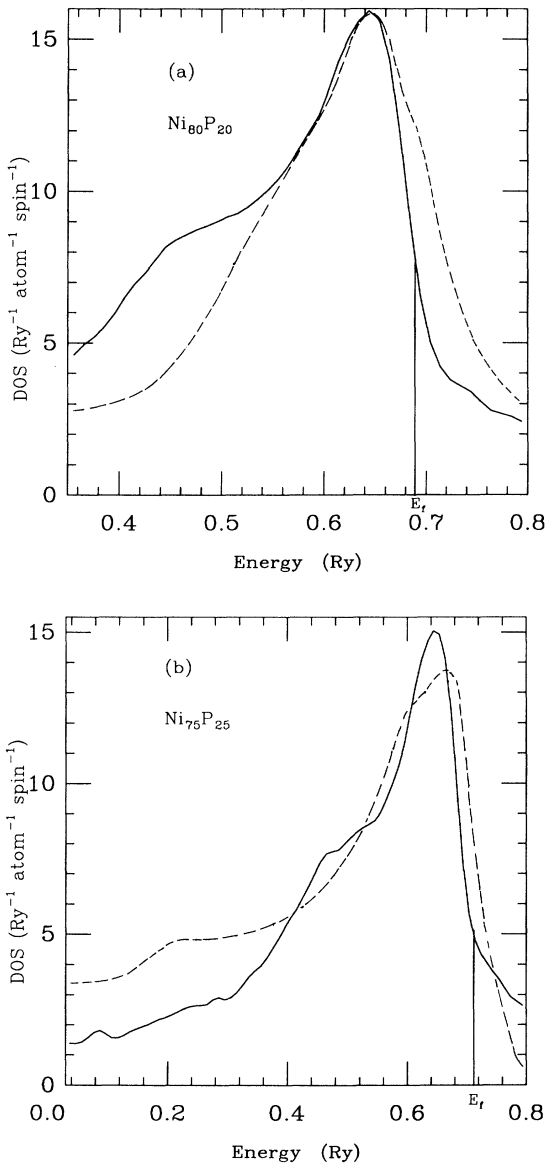

FIG. 2. Comparison of experimentally measured photoemission spectra with our calculated total DOS. (a) amorphous $Ni_{79}P_{21}$ data of Thube *et al.* (Ref. 17). (b) *crystalline* Ni_3P data of Amamou *et al.* (Ref. 18). The calculated results are the average from four computer-generated samples with 160 atoms each at each of the two concentrations. The energy is with respect to the muffin-tin zero. The Fermi energies of the experiments and the calculations have been lined up. The dashed lines are for experiment and the solid lines are for our calculations.

In Fig. 3 we compare our calculated DOS for $Ni_{80}P_{20}$ with an EMA calculation[19] and with a KKR-CPA calculation. (In the latter, it is assumed the atoms form a random alloy on a lattice.) Here the vertical scale as well as the energy scale (and location of the Fermi energy) are all determined by the respective calculations. Thus there are no adjustments in the scales of these curves. We see that there is good agreement among the three curves. There is more structure in the KKR-CPA DOS than in the other two calculations as one might expect, since the first is carried out on a lattice. However, it should be pointed out that, since our supercell is of finite size, the energy levels are discrete for this model. In order to simulate the results we would expect from a supercell of infinite size, we have broadened the discrete levels from the finite cell by a Gaussian broadening of width 0.01 Ry for our plots of the calculated DOS. Thus, our calculated results would not show any structure on the order of 0.01 Ry even if it were present in a model with an infinite supercell.

The total DOS as a function of energy near the Fermi energy is dominated by the Ni d-band density of states, as can be seen in the lower curves of Fig. 4 for $Ni_{80}P_{20}$. The Ni d-band DOS (the dashed curve) accounts for almost all of the total density of states (the solid curve) up to about 0.1 Ry above E_F. The contributions of the Ni s and p bands and the P s, p, and d bands are each less than one $Ry^{-1}atom^{-1}spin^{-1}$ over this range. These calculated results are averaged over the four samples of 160 atoms each; however the DOS graph for each individual sample is almost identical to the ensemble average at that concentration. The results for $Ni_{85}P_{15}$ and $Ni_{75}P_{25}$ are very similar.

Figure 5 shows our calculated total DOS in the vicinity of E_F for all three concentrations. We note that the Fermi energy increases both with respect to the muffin-tin

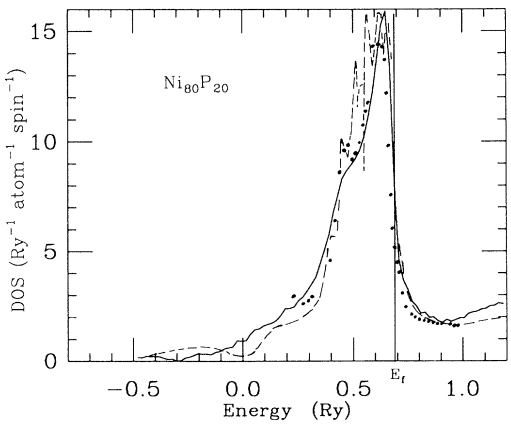

FIG. 3. Comparison of KKR-CPA and EMA density of states (for one spin) with our DOS calculation for $N_{80}P_{20}$. EMA spectra (Ref. 19) are based on Monte Carlo annealed pair distribution functions. The energy is relative to the muffin-tin zero. The dashed line is for the KKR-CPA calculation, the points are for the EMA calculation, and the solid line is for our present calculation. The EMA points on the upper edge of the d band are not fully converged.

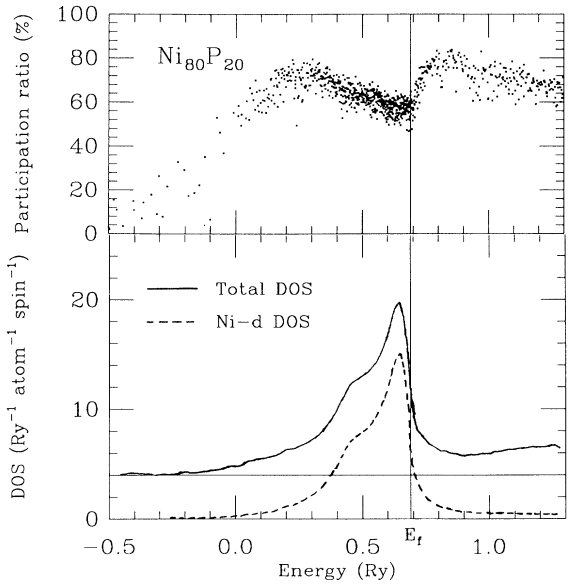

FIG. 4. Degree of localization (participation ratio) of each eigenstate (upper graph), total density of states for one spin (solid line), and Ni d-band density of states (dashed line) for our simulated $Ni_{80}P_{20}$ as a function of energy in Ry. The DOS results are the average of four samples with 160 atoms each. The participation ratio is given for only one of the four samples (one dot on the graph for each eigenstate). The vertical line indicates the Fermi energy. Note that the total DOS curve is displaced up 4 $(Ry\text{-}atom\text{-}spin)^{-1}$ units for clarity.

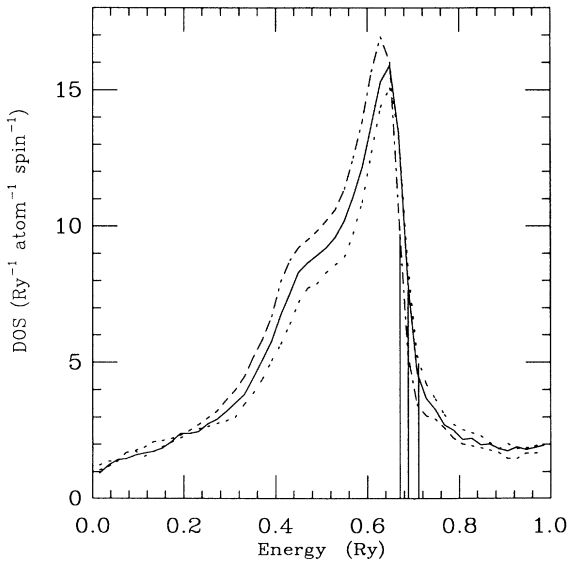

FIG. 5. The total density of states (for one spin) for the ensemble average over four samples of 160 atoms each of $Ni_{85}P_{15}$ (long dashes), $Ni_{80}P_{20}$ (solid curve), and $Ni_{75}P_{25}$ (short dashes) as a function of energy in Ry. The larger the concentration of Ni, the higher the peak. The vertical lines indicate the Fermi-energy level for each concentration. The left vertical line is E_F for $Ni_{85}P_{15}$, the middle vertical line is E_F for $N_{80}P_{20}$, while the right vertical line is E_F for $Ni_{75}P_{25}$.

zero and with respect to the peak in the DOS as phosphorus is added. Furthermore the DOS at the Fermi energy decreases with increasing P concentration.

These results are consistent with Knight-shift measurements[20,21] where it was found that the DOS at E_F decreases with increasing P concentration. Kuentzler, Bakonyi, and Lovas[22] have extracted the electronic DOS at E_F from their specific-heat measurements on $Ni_{81.5}P_{18.5}$, and they find 7.0 states per Ry per spin per atom. This compares with a DOS from our supercell calculation of 7.7 states per Ry per spin per atom at E_F for $Ni_{80}P_{20}$. According to our calculated results, the DOS at E_F is increasing rapidly with Ni concentration in this region. Thus we would expect a calculated DOS at E_F about 6% higher for 81.5% Ni than for 80.0% Ni. As discussed in Ref. 22, in extracting the electronic density of states from the specific-heat measurement, it was assumed that the contributions from the electron-electron interaction and the electron-phonon interaction are negligible. However, if these contributions are not negligible, then the part from the specific heat that should be compared with our calculated DOS would be smaller than 7.0 states per Ry per spin per atom. That is, in that case the divergence between the experimental and calculated DOS would be still larger.

According to Nagel and Tauc's nearly-free-electron model,[23] the relative stability of an amorphous metallic alloy against crystallization is related to the fact that the Fermi level E_F is located at a local minimum of the DOS. Our calculations do not support the free-electron model in that our calculated E_F lies at the steep edge of the Ni d band for all three concentrations.

According to Mott's s-d scattering model,[24] the dominant contribution to the resistivity of a metallic glass comes from the scattering of s,p electrons into d holes. Therefore, the resistivity should be proportional to the d electron DOS at E_F according to this model. But our calculated DOS at E_F is drastically decreased, and the experimental resistivity is increased as the P concentration increases. Hence our calculations, as well as the Knight-shift measurements[20,21] combined with resistivity measurements,[4,7] are not consistent with Mott's s-d scattering model.

An intuitive theoretical model for the electronic structure of metal-metalloid glasses is the rigid-band model. This model predicts that the addition of P atoms leads to electron-charge transfer from the P atoms to the Ni atoms that fill the Ni d band holes.[25] Since E_F in amorphous $Ni_{85}P_{15}$ (as well as in pure Ni) lies near the top of the Ni d band, such a filling would lead to an increase in E_F with a resulting decrease in the DOS at E_F. This decrease of the DOS at E_F with increasing P concentration is in qualitative agreement with our calculations and with the Knight-shift experiments.[20,21]

Since we have calculated the total number of electrons on each constituent atom and the angular-momentum-decomposed DOS, we can check the validity of the rigid-band model. The calculated average number of electrons on each Ni atom is almost the same for all three concentrations (and consequently is also nearly constant for P) as is the average number of d electrons on each Ni atom. In fact, contrary to the rigid-band model, a few Ni electrons are transferred to P atom sites as P is added in our calculations, and the number of d holes per Ni atom is nearly constant. This comes about because of a change in shape of the Ni d-band DOS with change of P concentration. One can see this in Fig. 5 where the total DOS is plotted. As already stated, these curves represent essentially the Ni d DOS. We see that the height of the peak decreases with increasing P, since the number of Ni atoms is decreasing. However above the Fermi level, the DOS increases (because the Ni d DOS in this region increases faster than the number of Ni atoms decreases) with increasing P. This increase in the Ni d DOS above the Fermi level compensates for the increase in the Fermi level so that the number of d holes per Ni atom is nearly constant. Therefore our calculations, as in earlier theoretical work[9-11] and experimental DOS studies by soft x-ray spectroscopy,[26] do not support the rigid-band model with charge transfer.

A question of interest is whether there is localization of the electronic states near the Fermi energy for materials with very strong disorder scattering such as in amorphous Ni-P alloys. Thus, we have determined the degree of localization of the eigenstates by calculating the participation ratio of each eigenstate. The participation ratio P_i for eigenstate $|i\rangle$ is defined to be

$$P_i = [N \sum_{n=1}^{N} |\langle n|i\rangle|^4]^{-1} ,$$

where N is the number of atoms in the supercell and $|n\rangle$ is the sum of the basis states centered on atom n. P_i takes values between zero and one, with zero (actually $1/N$) for a completely localized state and one for a completely extended state. Each mark in the top portion of Fig. 4 gives the participation ratio for a particular eigenstate of one of our 160 atom samples of $Ni_{80}P_{20}$. The other three samples at this concentration as well as those for the other concentrations give very similar results.

We see from this figure that the states in the middle of the Ni 3-d band are relatively more localized, while the Ni 3-d edge states are relatively delocalized because these latter states are strongly mixed with s and p states. Also, a few eigenstates at very low energy are localized. However, none of the states in the vicinity of the Fermi energy are localized in that the participation ratio is greater than 0.4 for all of these states and is greater than 0.5 for most of them. Localization due to the strong disorder scattering, would be evident in this model.

Because our model is of finite size, the eigenvalues are discrete, and one cannot obtain the zero-temperature dc resistivity directly. One way of getting around this problem is to calculate the resistivity at various nonzero frequencies and then extrapolate to zero frequency. We have done this using the one-electron approximation of the Kubo-Greenwood formula.[27,28] If one has a supercell that is periodically extended in space, then one has a perfect crystal (no matter what the disorder in the cell is) and hence one has an infinite conductivity. However, we use periodic boundary conditions only in determining the eigenvalues and eigenvectors of the electronic system in the finite-sized cell. For the Kubo conductivity we carry

out the integrals only over this finite space. For this calculation the conductivity is finite.

We take a configurational average (over four samples of 160 atoms each) of the resistivity as a function of frequency for a given atomic concentration, and these results with the standard deviations are plotted in Figs. 6. The standard deviations increase with decreasing frequency because with lower frequencies there are fewer of the discrete energy levels that can participate in the process. The resistivity data is fit to a Drude-type function $\rho(\omega)=\rho(0)+\beta\omega^2$ using least-squares-fitting methods.[29] This is the lower solid curve in each of Figs. 6. We see in Fig. 6(c) for $Ni_{75}P_{25}$ that our least-squares fit has a decreasing resistivity with frequency, which is in the opposite direction from what is usually expected. This peculiar behavior has the same origin as the Mooij correlation.[30] In fact the experimental temperature coefficient of resistivity is negative for $Ni_{75}P_{25}$. The zero-frequency ex-

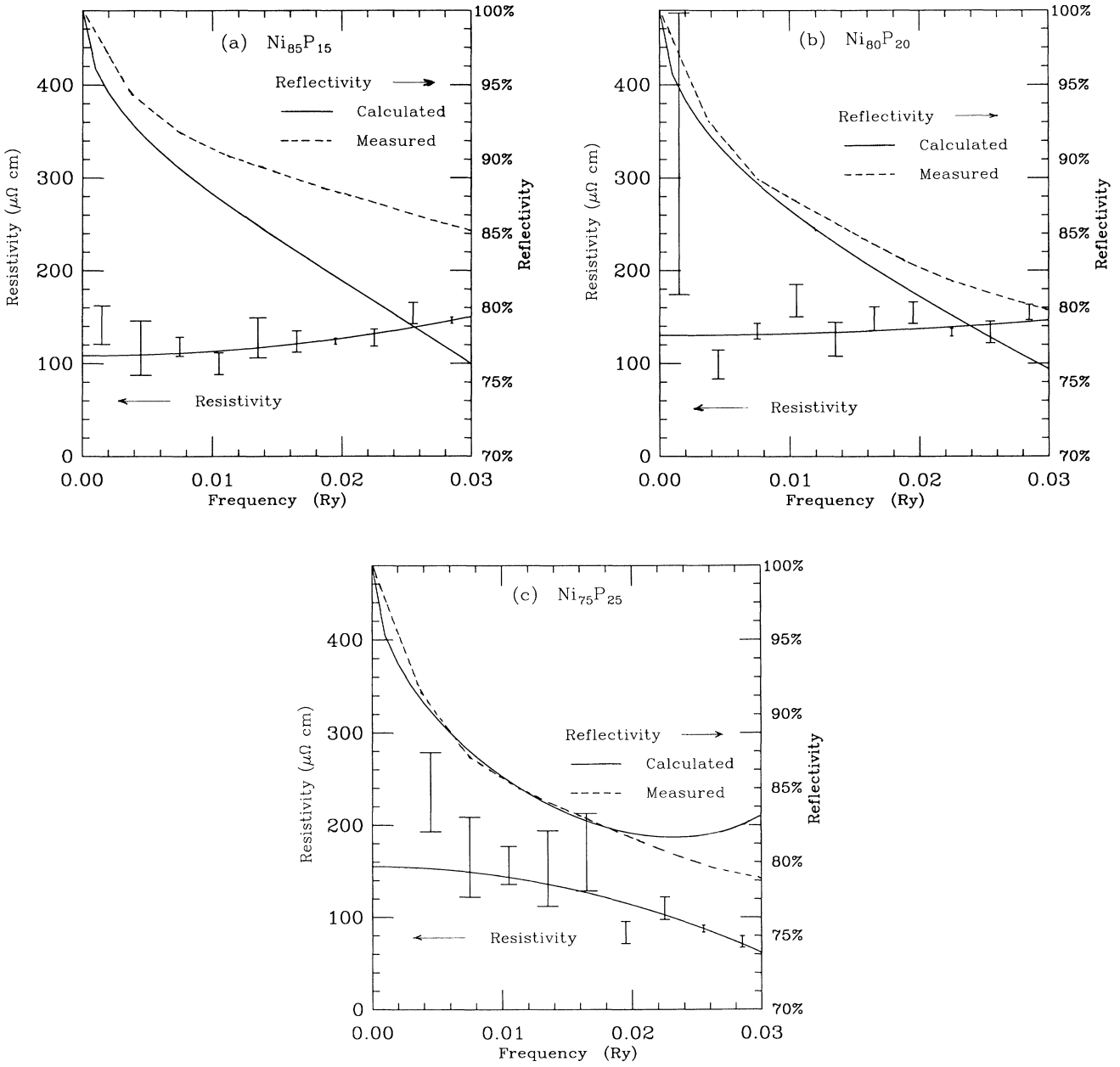

FIG. 6. Calculated resistivity (error bars) and reflectivity (upper solid curve) as a function of frequency in Ry for $Ni_{85}P_{15}$ (a), $Ni_{80}P_{20}$ (b), and $Ni_{75}P_{25}$ (c). The resistivity is fitted to $\rho(\omega)=\rho(0)+\beta\omega^2$ using least-squares-fitting methods (lower solid curve). The scale for the reflectivity is to the right. The experimentally measured reflectivity (dashed curve) is for $Ni_{84.8}P_{15.2}$, $Ni_{78.9}P_{21.1}$, and $Ni_{73.8}P_{26.2}$ (Ref. 32).

trapolations of the least-squares fits determine the dc resistivities.

We found large standard deviations in the resistivity calculations for 80 atoms per unit cell indicating that a cell size of 80 atoms is not large enough to calculate reliable resistivities.[31]

The dc data are plotted in Fig. 7. We see that the calculated dc resistivity values agree within statistical fluctuations and experimental error with the experimentally measured values[4,7] except for $Ni_{85}P_{15}$ in which case the calculated resistivity is slightly higher than experiment, lying somewhat outside the combined statistical fluctuation and experimental error range.

There may be a trend in our calculations to give somewhat too small a change in resistivity with change in concentration. However this is right at the edge of the accuracy of the calculations and of the experiments. Our calculated resistivities are at zero temperature. We have then used the experimental values of the temperature dependence of the resistivities to convert our zero-temperature results to room-temperature numbers for Fig. 7. However, the disorder scattering is such a large part of the total resistivity that the resistivity changes at most 5% in going from zero temperature to room temperature.

Using the Drude least-squares fit to the resistivities as a function of frequency (the lower curves in Fig. 6), we have calculated the reflectivity as a function of frequency for the three concentrations. In these calculations we have assumed that the imaginary part of the resistivity is negligible. The calculated reflectivities as a function of frequency are plotted as the upper solid curve in each of Figs. 6. The differences between the calculated and measured reflectivities[32] are less than 5% for $Ni_{75}P_{25}$ and $Ni_{80}P_{20}$. However, the differences between our calculation and experiment for $Ni_{85}P_{15}$ as a function of frequency are as large as 9%. In the experiments,[32] the reflectivities for 21.1 at. % P and for 26.2 at. % P are almost identical over the frequency range from zero to 0.5 eV (0.0367 Ry—the frequency range we are interested in, in our work), whereas there are relatively large differences between the measured reflectivities for 21.1 at. % P and 26.2 at. % P on the one hand and 15.2 at. % P on the other. However the measured dc resistivities[4,7] indicate that the difference between 15 at. % P and 20 at. % P should be comparable to or even smaller than the difference between 20 at. % P and 25 at. % P. Because reflectivity is closely related to the resistivity, we do not believe the relatively large difference in the experimental reflectivity of 15.2 at. % P and the other two concentrations is a real effect. Thus we are not concerned with the larger deviation of our calculated results from the experiments for the 15 at. % P sample compared to the deviations for 20% and 25 at. % P.

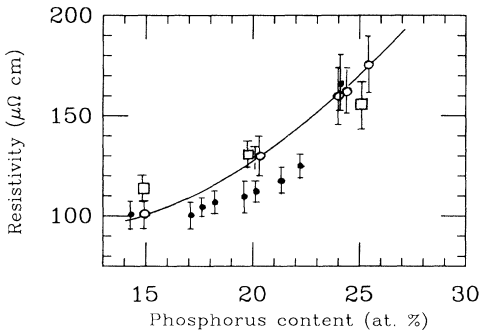

FIG. 7. Experimentally measured dc resistivity at room temperature (Ref. 4, solid circles and Ref. 7, open circles and solid line) and our calculated resistivity (open squares). The calculated resistivity is converted to room temperature using the experimentally measured temperature dependence of the resistivity (Ref. 7).

V. CONCLUSIONS

We have simulated the Ni-P amorphous alloy system for three concentrations, and have calculated the total density of states, component- and angular-momentum-decomposed density of states, degree of localization (participation ratio), and current matrix elements for the electrons. We also have calculated the electrical resistivity and reflectivity as a function of frequency and concentration using the Kubo formula, and have compared our calculated results with experiment. In the DOS calculations, the calculated results for both the 80 and 160 atom cases agree with photoemission data as to the location and shape of the main peak. We find good agreement between our calculated DOS and results obtained from the effective medium approximation and KKR-CPA.

In these supercell calculations for the electronic properties for the Ni-P amorphous alloys, we have included angular-momentum-decomposed eigenfunctions up to $l=2$. To check on the contribution of higher l values, we have carried out KKR-CPA resistivity calculations for Ni-P random substitutional alloys (assuming the atoms reside at random on an fcc lattice) at the same three concentrations both for $l_{\max}=2$ and for $l_{\max}=3$. The results of these calculations show that the resistivity change on increasing the maximum angular momentum to $l=3$ is of the order of 8%–20%, depending on the concentration. Thus we believe that our amorphous-alloy model is reasonably well converged at $l_{\max}=2$. Therefore, we believe our LKKR-supercell calculation of the resistivity with $l_{\max}=2$ for Ni-P amorphous alloy system is valid to about 10%.

Taking into account the standard deviations due to the fluctuations in our calculated resistivities over the four samples together with the experimental error, our calculated resistivities for the 160 atom cases agree with experiment. However the 80 atom supercells are too small to have the statistical fluctuations as low as the experimental errors.[31] The change in our calculated resistivity with concentration may be slightly smaller than that found experimentally, but the combination of the standard deviations in the calculations and the experimental errors in the measurements make it impossible to determine this for certain. On the other hand, our KKR-CPA resistivities for Ni-P for the same three concentrations are

21–48 % lower than the resistivities from our supercell calculations and from experiment. For these calculations we find that for $l_{max}=2$, the KKR-CPA resistivity goes from 79 $\mu\Omega$ cm at 15% P to 89 $\mu\Omega$ cm at 25% P. In addition to giving resistivities that are much too low at each concentration, the KKR-CPA results do not give the required large variation of resistivity with concentration. Thus, to get reasonable agreement with experiment, it is necessary for the model to have structural disorder. It is not enough to have only chemical disorder on a lattice.

There are other calculations that should be done in the future. We think it would be useful to calculate the resistivity as a function of temperature and the thermopower as a function of concentration, since the experimental temperature coefficient of resistivity becomes negative (Mooij correlation[30]) for P concentrations higher than 23%,[4] while the experimental thermopower changes sign and becomes positive, also for P concentrations greater than 18%.[4]

ACKNOWLEDGMENTS

We wish to acknowledge valuable conversations with D. B. Baxter, W. H. Butler, J. P. Carini, S. M. Girvin, R. G. Newton, and W. L. Schaich. We also wish to thank John Connolly for his hospitality at the Workshops on Computational Methods for the Structure of Alloys at the University of Kentucky, where we benefited from stimulating interactions with many of the participants. H.J.Y. and J.C.S. were supported by National Science Foundation (NSF) Grant No. DMR-8701583. The research of D.M.N. and R.H.B. was sponsored by Department of Energy (DOE), Assistant Secretary for Conservation and Renewable Energy, Office of Industrial Technologies, Advanced Industrial Concepts Materials Program under Contract No. DE-AC05-84OR21400 with Martin Marietta Energy Systems, Inc. Many of the calculations of this work were carried out on the CRAY–XMP and CRAY-2 at the National Center for Supercomputing Applications, Champaign, Illinois.

[1] *Glassy Metals I and II*, edited by H. J. Guntherodt and H. Bec (Springer-Verlag, New York, 1981 and 1983).

[2] *Binary Alloy Phase Diagrams*, edited by T. B. Massalski (American Society for Metals, Metals Park, Ohio, 1986).

[3] G. S. Cargill III, J. Appl. Phys. B **23**, 315 (1976).

[4] J. P. Carini, S. R. Nagel, L. K. Varga, and T. Schmidt, Phys. Rev. B **27**, 7589 (1983).

[5] L. H. Bennett, H. E. Schone, and P. Gustafson, Phys. Rev. B **18**, 2027 (1978).

[6] S. W. McKnight and A. K. Ibrahim, Phys. Rev. B **29**, 6570 (1984).

[7] P. J. Cote, Solid State Commun. **18**, 1311 (1976); P. J. Cote and L. V. Meisel, Phys. Rev. B **20**, 3030 (1979).

[8] For a review, see D. G. Naugle, J. Phys. Chem. Solids **45**, 367 (1984).

[9] W. Y. Ching, Phys. Rev. B **34**, 2080 (1986); J. Non-Cryst. Solids **75**, 379 (1985).

[10] S. N. Khanna, A. K. Ibrahim, S. W. McKnight, and A. Bansil, Solid State Commun. **55**, 223 (1985).

[11] M. R. Press, S. N. Khanna, and P. Jena, Phys. Rev. B **36**, 5446 (1987).

[12] T. W. Weber and F. H. Stillinger, Phys. Rev. B **31**, 1954 (1985); *ibid.* **32**, 5402 (1985).

[13] P. Lamparter and S. Steeb, in *Rapidly Quenched Metals*, edited by S. Steeb and H. Warlimont (Elsevier, Amsterdam, 1985), p. 459.

[14] Hyungjin Yang, Ph.D. thesis, Indiana University, 1990 (unpublished).

[15] J. S. Faulkner and T. P. Beaulac, Phys. Rev. B **26**, 1597 (1982).

[16] We have carried out some calculations on 300 atom samples. Our preliminary results indicate that the shape of the DOS has not changed, that E_F has changed by a few tenths of a percent, and that the DOS at E_F differs by about 6% from the corresponding 160 atom models.

[17] M. G. Thube, S. K. Kulkarni, D. Huerta, and A. S. Nigavekar, Phys. Rev. B **34**, 6874 (1986).

[18] A. Amamou, D. Aliaga-Guerra, P. Panissod, G. Krill, and R. Kuentzler, J. Phys. (Paris) Colloq. **41**, C8-396 (1980).

[19] A. Chowdhary, D. M. Nicholson, and L. M. Schwartz, J. Non-Cryst. Solids **76**, 147 (1985).

[20] W. A. Hines, C. U. Modzelewski, R. N. Paolino, and R. Hasegawa, Solid State Commun. **39**, 699 (1981).

[21] D. S. Lashmore, L. H. Bennet, H. E. Schone, P. Gustafson, and R. E. Watson, Phys. Rev. Lett. **48**, 1760 (1982).

[22] R. Kuentzler, I. Bakonyi, and A. Lovas, Solid State Commun. **55**, 567 (1985).

[23] S. R. Nagel and J. Tauc, Phys. Rev. Lett. **35**, 380 (1975).

[24] N. F. Mott, Philos. Mag. **26**, 1249 (1972).

[25] D. E. Polk, Scr. Metall. **4**, 117 (1970).

[26] E. Belin, C. Bonnelle, J. Flechon, and F. Machizaud, J. Non-Cryst. Solids **41**, 219 (1980).

[27] R. Kubo, J. Phys. Soc. Jpn. **12**, 570 (1957).

[28] D. A. Greenwood, Proc. Phys. Soc. London **71**, 585 (1958).

[29] W. H. Press, B. P. Flannery, S. A. Teukolsky, and W. T. Vetterling, *Numerical Recipes* (Cambridge University Press, Cambridge, England, 1986), pp. 509–515.

[30] J. H. Mooij, Phys. Status Solidi A **17**, 521 (1973).

[31] The differences between the dc resistivities averaged over four samples of 80 atoms each and 160 atoms each are less than one standard deviation of the 80 atom cases. However this standard deviation for 80 atoms is quite large for each concentration. Preliminary results on 300 atom cells (Ref. 16) indicate that the dc resistivities for these larger samples are within 12 to 18% of the results for the 160 atom cases.

[32] S. W. McKnight and A. K. Ibrahim, J. Non-Cryst. Solids **61**, 1301 (1984).